ISCRA 2019
International Symposium on Cosmic Rays and Astrophysics
25 – 28 June 2019
National Research Nuclear University MEPhI
(Moscow Engineering Physics Institute), Moscow, Russia

METHOD OF GLOBAL SURVEY BY DATA OF MUON TELESCOPES

V.G. Grigoryev[1] , P.Yu. Gololobov[1], P.A. Krivoshapkin[1] , G.F. Krymsky[1], S.A. Starodubtsev[1], A.S. Zverev[1], V.G. Yanke [2]

1 Yu.G. Shafer Institute of Cosmophysical Research and Aeronomy Federal Research Centre "Yakutsk Scientific Centre of Siberian Branch of the Russian Academy of Sciences" Separate Subdivision

2 Institute of Terrestrial Magnetism, Ionosphere and Radio Wave Propagation after N.V. Pushkov of the Russian Academy of Sciences

Introduction. Global Survey Method

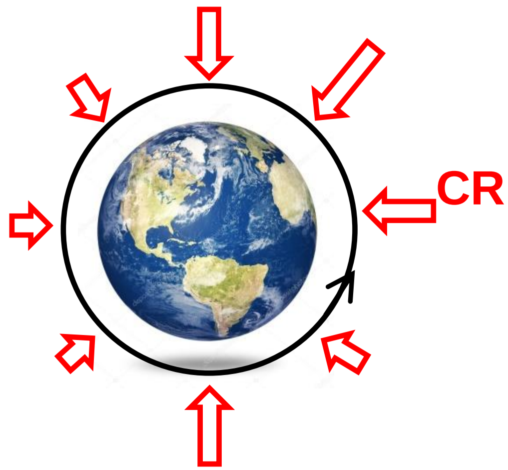

Global Survey Method (ShICRA, Yakutsk, Russia)
A.M. Altukhov, G.F. Krymsky, A.I. Kuzmin et al., *Proc. 11th ICRC*, **TE-15**, 1969

Global Survey Method (IZMIRAN, Troitsk, Russia)
A.V. Belov, E.A. Eroshenko, V.G. Yanke et al. *Geomagnetism and Aeronomy*, **58**, 2018

Global Spectrographic Survey Method (ISTP, Irkutsk, Russia)
V.M. Dvornikov, V.E. Sdobnov. *Solar Physics*, **178**, 1998

3-D CR anisotropy (Nagoya, Japan)
K. Nagashima et al. *Rep. Ionos. Space Res.*, **25**, 1971

Space Weather + *Real-time* **Neutron Monitor Data Base** = **Forecasting**

http:/www.nmdb.eu

MT data???

GMDN team

K. Munakata et al. *J. Geophys. Res.*, **105,** 2000
T. Kuwabara et al., *Space Weather*, **4**, 2006
K. Munakata et al. *Geophys. Res. Lett.*, **32**, 2005
M. Rockenbach et al. *Geophys. Res. Lett.*, **38**, 2011
……

ICME geometry, searching for precursors of geomagnetic disturbances et al.

Database used in the project.

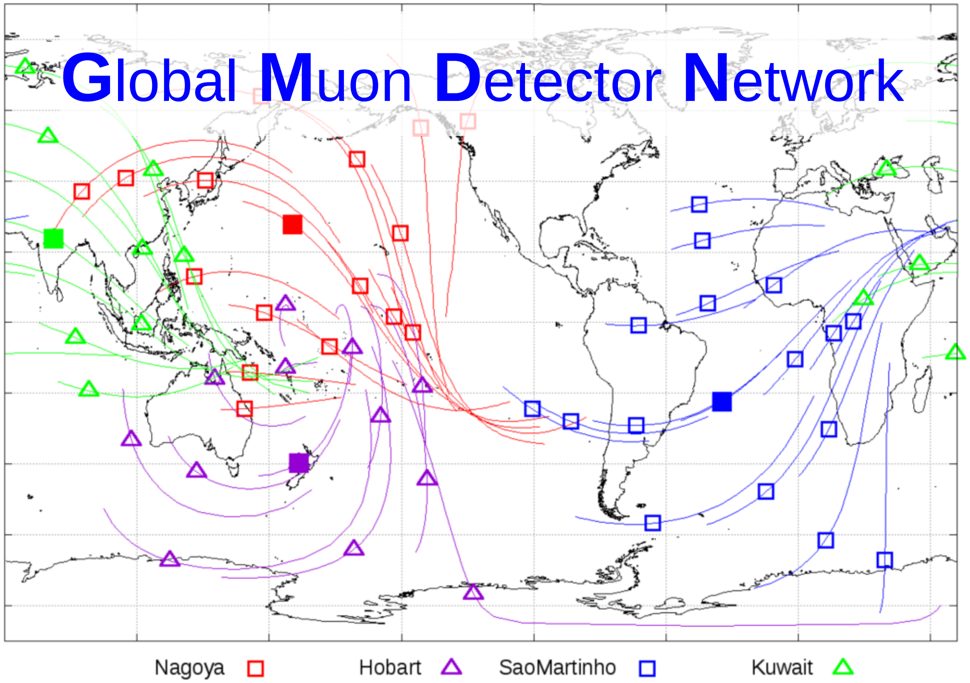

Figure 2.1. Asymptotic viewing directions of 60 channels of the GMDN. [M. Kozai, 2016]

Station	The size of detector, m^2	Number of directions	Pm (GV)
Nagoya	6×6	17	58.4~106.9
Hobart	4×4	13	53.1~74.0
Sao-Martinho	4×8	17	54.3~98.4
Kuwait	4.3×5.0	13	59.8~94.5
Yakutsk	2.7×1.3	3	~50-60

Table. Characteristics of the GMDN. [K. Munakata et al., The Astrophys. J., 2018]

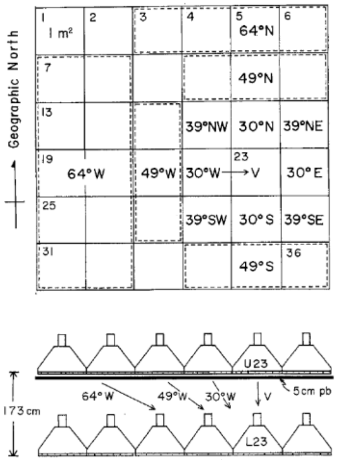

← Figure 2.2. Typical construction of multi-directional muon telescope (as an example Nagoya construction is presented). [http://www.stelab.nagoya-u.ac.jp/ste-www1/div3/muon/dbtext22.pdf]

Global muon detector network **GMDN**
http://cosray.shinshu-u.ac.jp/crest/DB/Public/Archives/GMDN.php
+ 3 directions of Yakutsk muon telescope **MT-00**
The data and acceptance characteristics are presented through the links
http://www.ysn.ru/ipm/
http://www.hecrlab.ysn.ru/index.php/en/

Temperature effect

was eliminated by the method developed by IZMIRAN team
[M.G. Kostyuk, V.B. Petkov, R.V. Novoseltseva et al. *Bull. of RAS: Phys.*, **77**, 2013]

Global Survey Method

CR intensity in free space

$$I(\theta,\phi) = \sum_{n=0}^{\infty}\sum_{m=0}^{n}\left(a_n^m \cdot \cos(m\phi) + b_n^m \cdot \sin(m\phi)\right) P_n^m(\sin\theta)$$

$$I_j = \sum_{n=0}^{\infty}\sum_{m=0}^{n}\left(a_n^m \cdot x_{n,j}^m + b_n^m \cdot y_{n,j}^m\right) k_n^{(j)} \qquad k_n^{(j)} = \frac{\int_{\varepsilon_{min}}^{\infty} W^i(E) f_n(E) dE}{\int_{E_{min}}^{\infty} W^0(E) f_n(E) dE}$$

Receiving vectors («coupling coefficients»)

$$Z_n^m = \frac{\int_{E_{min}}^{\infty}\int_0^{2\pi}\int_0^{\pi/2} W(E) f_n(E) N(\theta,\phi)\sin(\theta) e^{im\psi(E,\theta,\phi)} P_n^m\left(\sin\Phi(E,\theta,\phi)\right) dE\, d\theta\, d\phi}{\int_{E_{min}}^{\infty}\int_0^{2\pi}\int_0^{\pi/2} W(E) f_n(E) N(\theta,\phi)\sin(\phi) dE\, d\theta\, d\phi}$$

$$\vec{\boldsymbol{A}} = (a_0^0, a_1^0, a_1^1, b_1^1, a_2^0, a_2^1, b_2^1, a_2^2, b_2^2, ..) \qquad \vec{\boldsymbol{Z}} = (x_0^0, x_1^0, x_1^1, y_1^1, x_2^0, x_2^1, y_2^1, x_2^2, y_2^2, ..)$$

$$\overrightarrow{\boldsymbol{I_{obs}}} = \widehat{\boldsymbol{M}} \cdot \vec{\boldsymbol{A}} \quad \Rightarrow \quad \vec{\boldsymbol{A}} = \left(\widehat{\boldsymbol{M}}^T \cdot \widehat{\boldsymbol{M}}\right)^{-1} \widehat{\boldsymbol{M}}^T \cdot \overrightarrow{\boldsymbol{I_{obs}}}$$

$\widehat{\boldsymbol{M}}$ - matrix of receiving vectors

$\vec{\boldsymbol{A}}$ - multidimentional vector of CR distribution in free space

$\overrightarrow{\boldsymbol{I_{obs}}}$ - observed by the MT network diurnal and semidiurnal variations of CR at the Earth

$$\Delta = \overrightarrow{\boldsymbol{I_{obs}}} - \widehat{\boldsymbol{M}} \cdot \vec{\boldsymbol{A}} \qquad \boldsymbol{B}_\Delta = \Delta \cdot \Delta^{\boldsymbol{T}} = [\boldsymbol{1} - \boldsymbol{M}\left(\boldsymbol{M}^{\boldsymbol{T}}\boldsymbol{M}\right)^{-\boldsymbol{1}}\boldsymbol{M}^{\boldsymbol{T}}]\boldsymbol{\sigma}^{\boldsymbol{2}} \qquad \boldsymbol{\sigma}^{\boldsymbol{2}} = \frac{\Delta \cdot \Delta^{\boldsymbol{T}}}{\boldsymbol{N} - \boldsymbol{n}}$$

[A.M. Altukhov, G.F. Krymsky, A.I. Kuzmin et al., *Proc. 11th ICRC*, **TE-15**, 1969]

Approximate Formula for Response Function of Cosmic Ray Hard Component at Various Depths of the Atmosphere and Underground *Energy distribution of primary cosmic ray nucleons responsible for muons detected at sea level and underground*

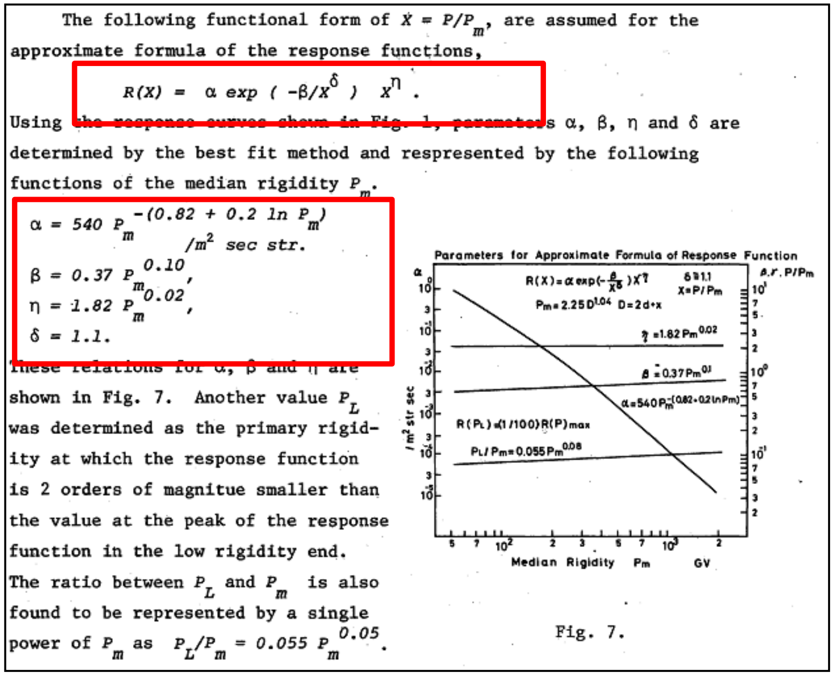

The following functional form of $X = P/P_m$, are assumed for the approximate formula of the response functions,

$$R(X) = \alpha \exp(-\beta/X^{\delta})\ X^{\eta}.$$

Using the response curves shown in Fig. 1, parameters α, β, η and δ are determined by the best fit method and respresented by the following functions of the median rigidity P_m.

$$\alpha = 540\ P_m^{-(0.82 + 0.2 \ln P_m)}\ /m^2\ \mathrm{sec\ str.}$$
$$\beta = 0.37\ P_m^{0.10},$$
$$\eta = 1.82\ P_m^{0.02},$$
$$\delta = 1.1.$$

These relations for α, β and η are shown in Fig. 7. Another value P_L was determined as the primary rigidity at which the response function is 2 orders of magnitude smaller than the value at the peak of the response function in the low rigidity end. The ratio between P_L and P_m is also found to be represented by a single power of P_m as $P_L/P_m = 0.055\ P_m^{0.05}$.

Fig. 7.

Figure 4.1. The fragment from the work [K. Fujimoto, K. Murakami, I. Kondo, K. Nagashima et al.// *Proc. 15th ICRC, Plovdiv, Bulgaria*, 1977]

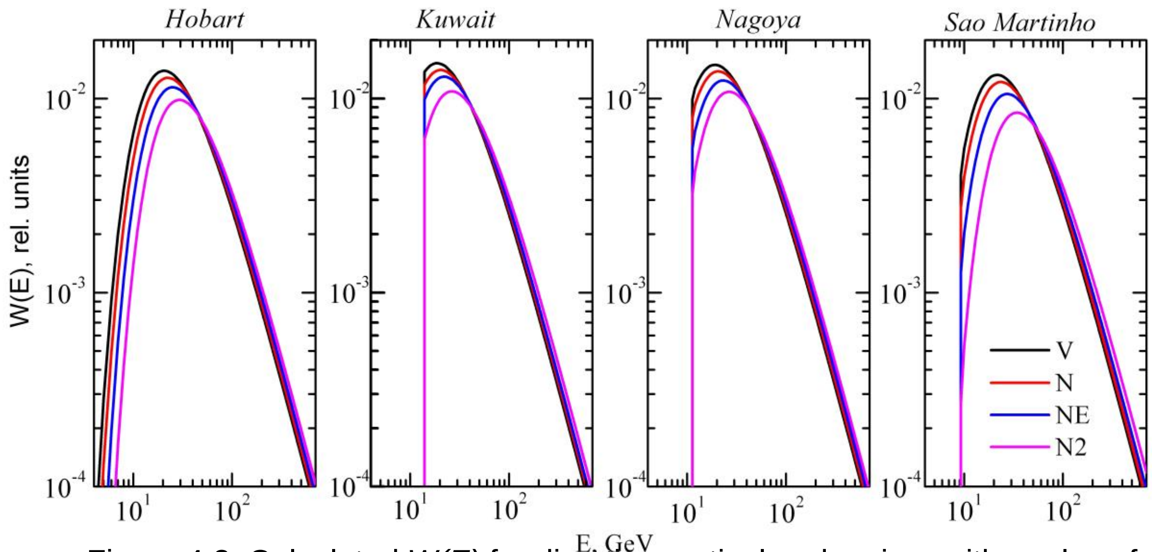

Figure 4.2. Calculated *W(E)* for direction vertical and main zenith angles of registration.

[Das & De, 1980] shows a good agreement.

GMDN Acceptance characteristics. Directional sensitivities

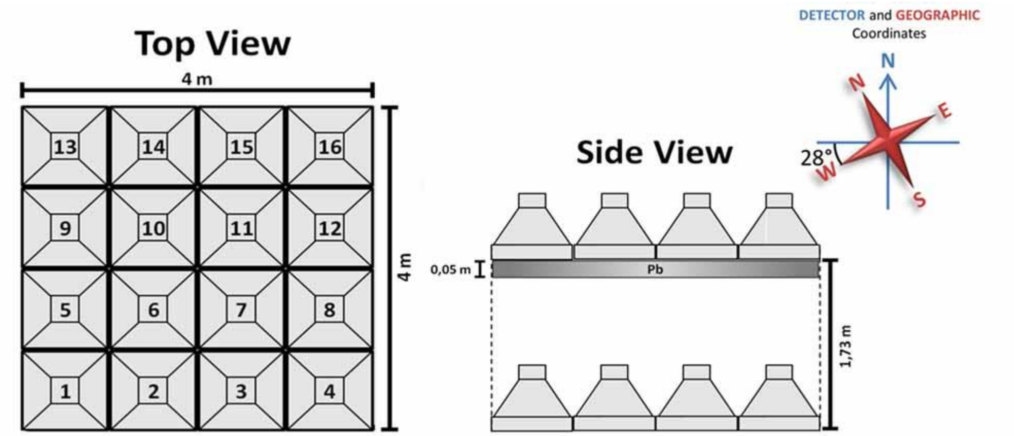

Figure 5.1. Hobart MT geometry. Example of PS (Plastic scintillator) type MT.

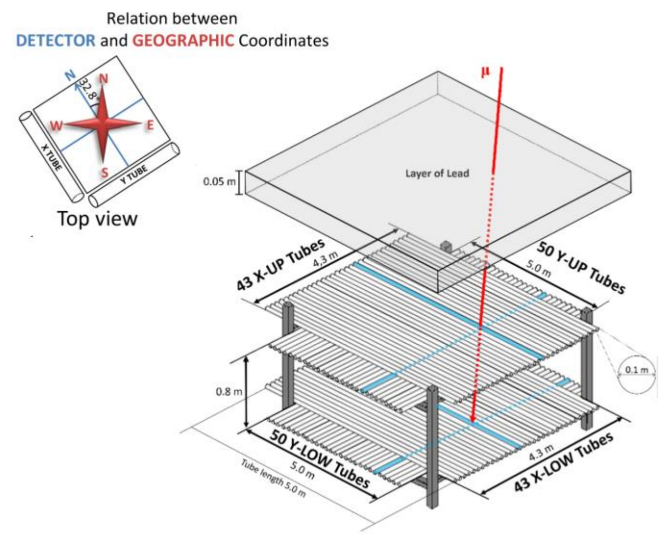

Figure 5.3. Kuwait MT geometry. Example of PCT (Proportional counter tube) type MT.

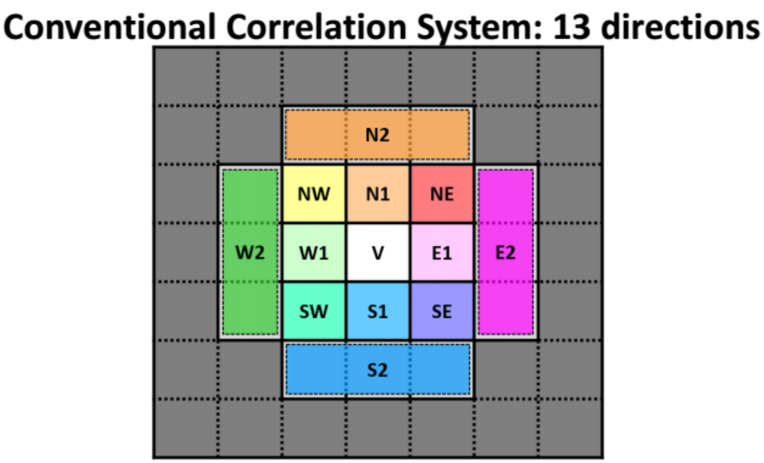

Figure 5.2. Conventional correlation system of Hobart MT
[http://cosray.shinshu-u.ac.jp/crest/DB/Public/Archives/GMDN.php]

GMDN Acceptance characteristics. Directional sensitivities

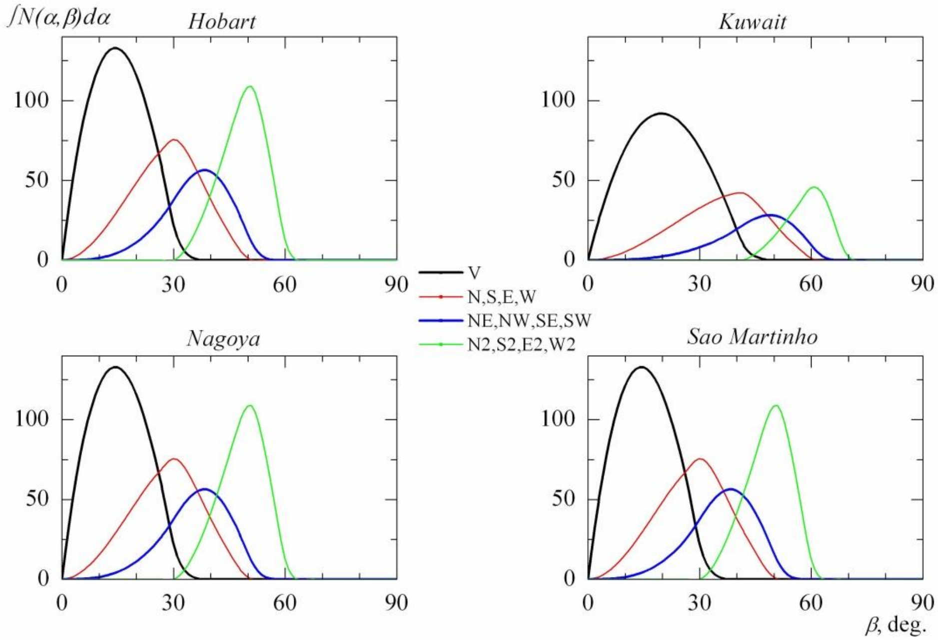

Figure 6.1. Directional sensitivity of the channels of the GMDN with respect to zenithal angle

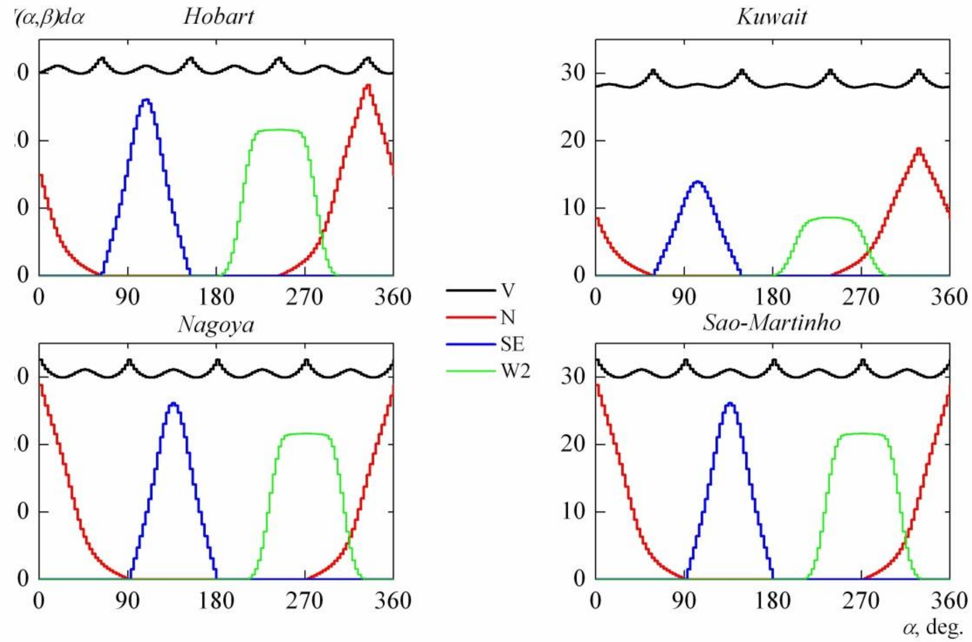

Figure 6.2. Directional sensitivity of the channels of the GMDN with respect to azimuthal angle

The principle construction is presented in [http://cosray.shinshu-u.ac.jp/crest/DB/Public/Archives/GMDN.php]

Calculated acceptance characteristics for the GMDN are available through the link
http://www.ysn.ru/smt

GMDN Acceptance characteristics. Trajectories of CR in the magnetosphere.

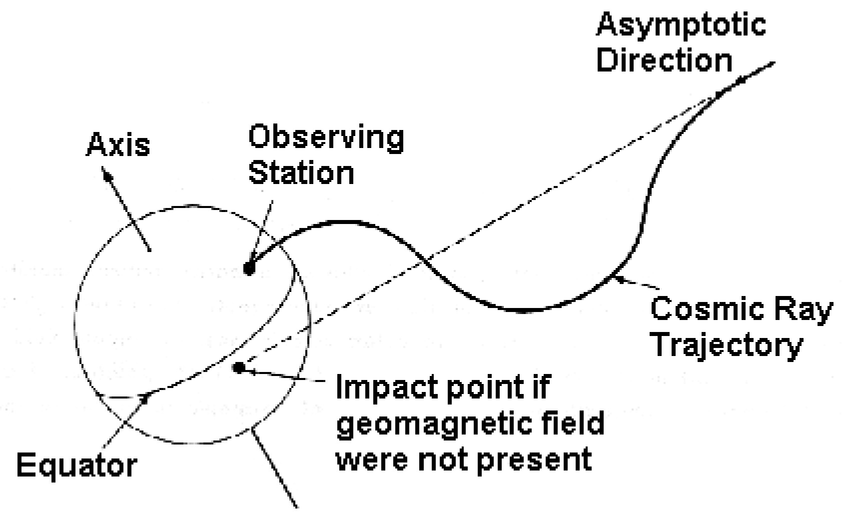

Figure 7. Schematic illustration of CR particle trajectory in the magnetosphere [http://neutronm.bartol.udel.edu/catch/cr2.html]

$$V(r,\theta,\phi,t) = a\sum_{n=1}^{N}\sum_{m=0}^{n}\left(\frac{a}{r}\right)^{n+1}\left[g_n^m(t)\cos(m\phi) + h_n^m(t)\sin(m\phi)\right]P_n^m(\cos\theta)$$

International Geomagnetic Reference Field IGRF-10
Based on 10 first spherical harmonics
https://www.ngdc.noaa.gov/IAGA/vmod/igrf.html

tracking of particle is made according to [Dorman, Smirnov, Tyasto, 1971]

Calculated acceptance characteristics for the GMDN are available through the link http://www.ysn.ru/smt

GMDN Acceptance characteristics. Energy spectra & receiving vectors

Energy spectrum for first and second spherical harmonics:

$$\begin{cases} f_1(\varepsilon) = const, & \text{if} \quad \varepsilon \le E_0 \\ f_1(\varepsilon) = 0, & \text{if} \quad \varepsilon > E_0 \end{cases}$$

where E_0 = 40, 60, 80, 100 GeV.

$$\begin{cases} f_2\left(\dfrac{\varepsilon}{E_0}\right)^2, & \text{if} \quad \varepsilon \le E_0 \\ f_2\left(\dfrac{\varepsilon}{E_0}\right)^{-1}, & \text{if} \quad \varepsilon > E_0 \end{cases}$$

where E_0 = 50, 70, 100, 150 GeV.

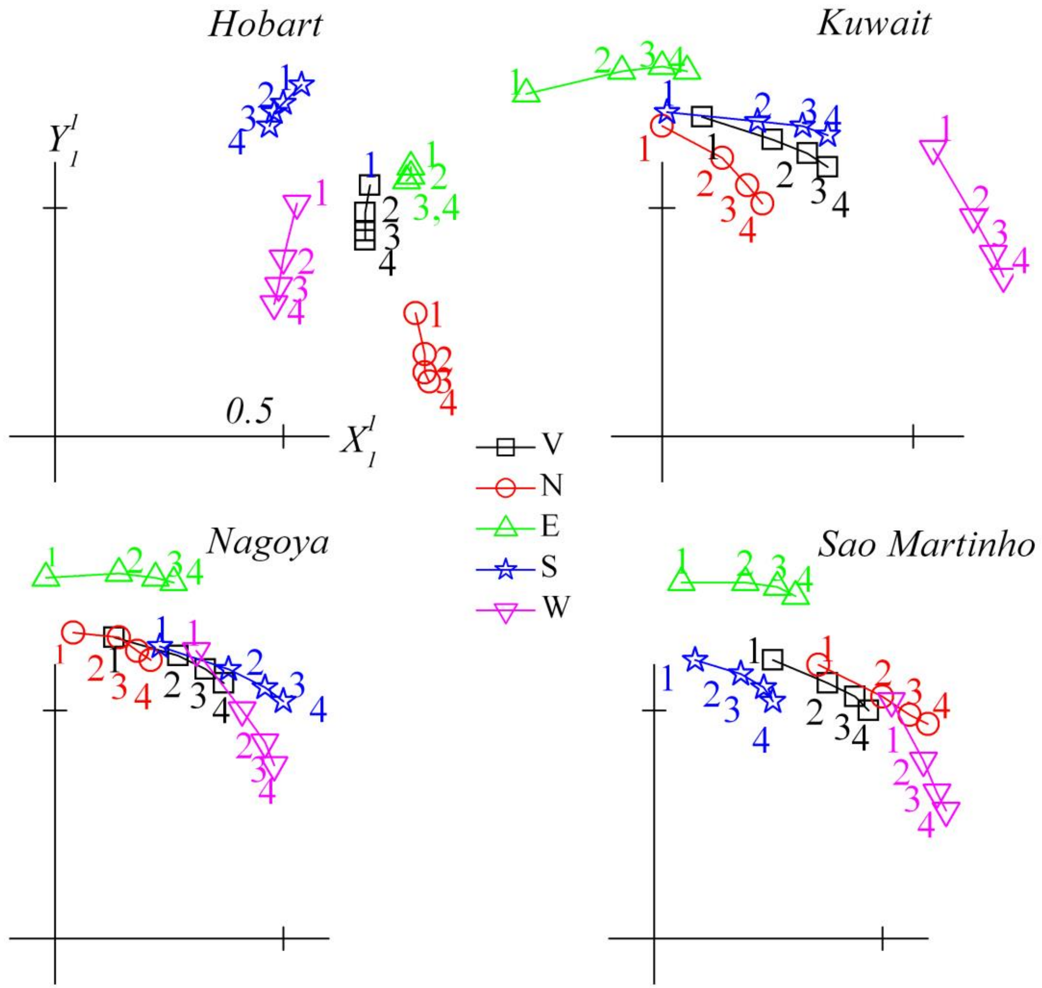

Figure 8. Calculated receiving vectors of diurnal variation $\overline{Z_1^1} = (X_1^1, Y_1^1)$ for GMDN stations for different spectrums

Calculated acceptance characteristics for the GMDN are available through the link
http://www.ysn.ru/smt

Preliminary results of GSM practical application

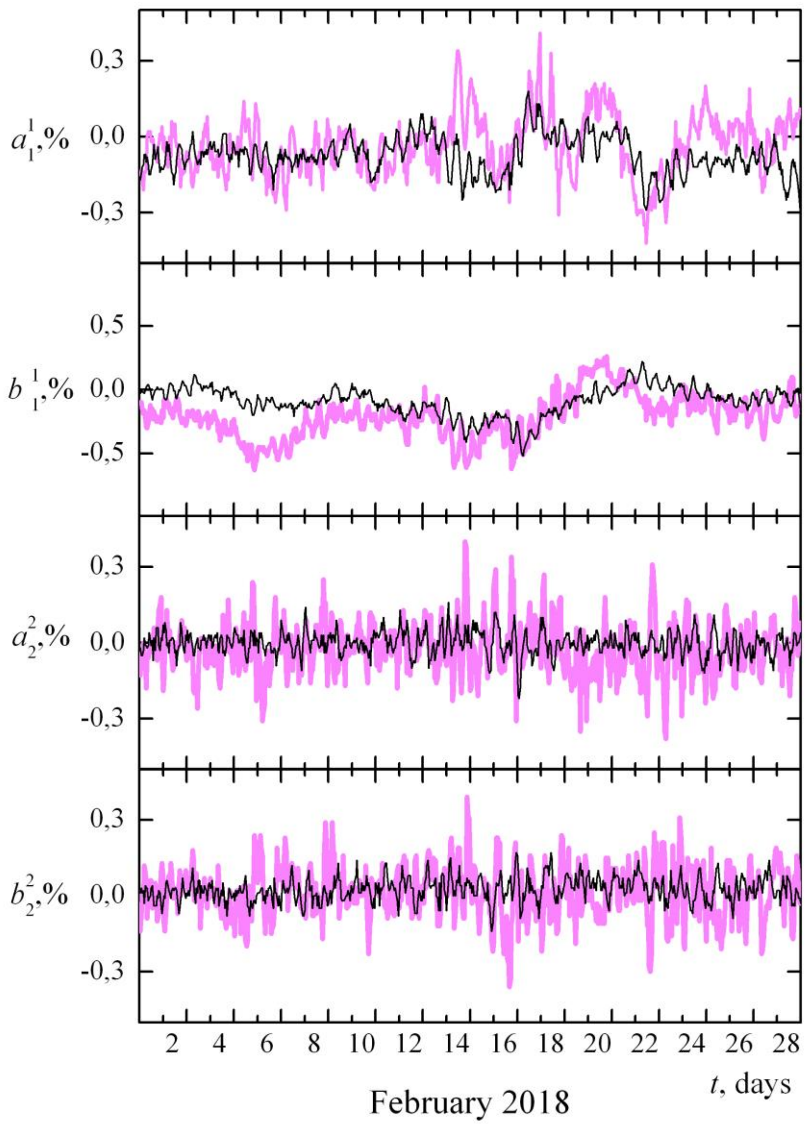

Figure 9.1. Comparison of the components of diurnal variation of CR obtained by both MT and NM

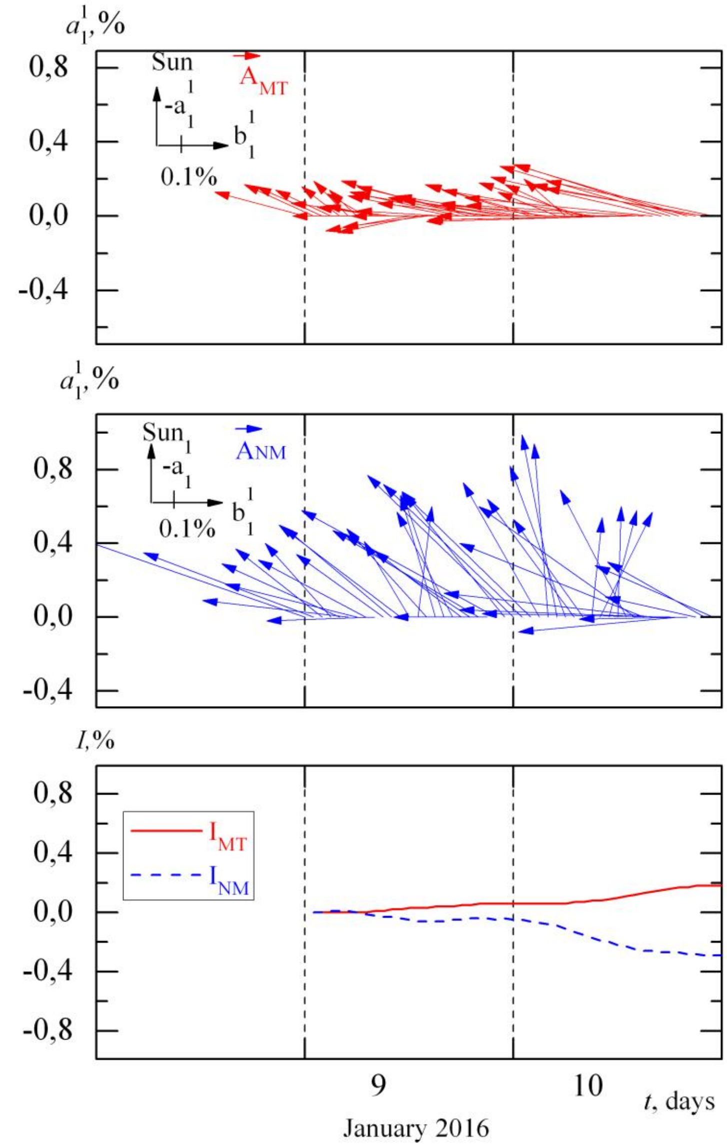

Figure 9.2. Behavior of a vector of diurnal variation obtained by GSM by data of MT and NM.

Conclusion

1. The new variant of the Global Survey Method that is based on the data of the world network of muon telescopes is developed.
2. Preliminary results of the analysis of the obtained parameters of CR distribution show that the method provides reliable and informative data. The method is expected to provide a new information on the structure and the dynamic of the heliosphere.
3. The obtained acceptance characteristics for the GMDN are available through the link [http://www.ysn.ru/smt]

The work was carried out under the support of RFBR grant No. 18-02-00451-a using an USD SCR network. Also, we gratefully thanks to authors of NMDB, MDDB and GMDN databases for providing their data.

THANK YOU FOR YOUR ATTENTION!

The work was carried out under the support of RFBR grant No. 18-02-00451-a using an USD SCR network. Also, we gratefully thanks to authors of NMDB, MDDB and GMDN databases for providing their data.